

The spectrum of qubitized QCD: glueballs in a $S(1080)$ gauge theory

Andrei Alexandru,^{1,2,*} Paulo F. Bedaque,^{2,†} Ruairí Brett,^{1,‡} and Henry Lamm^{3,§}

¹*Physics Department, The George Washington University, Washington, DC 20052, USA*

²*Department of Physics, University of Maryland, College Park, MD 20742, USA*

³*Fermi National Accelerator Laboratory, Batavia, Illinois, 60510, USA*

(Dated: December 17, 2021)

Quantum simulations of QCD require digitization of the infinite-dimensional gluon field. Schemes for doing this with the minimum amount of qubits are desirable. We present a practical digitization for $SU(3)$ gauge theories via its discrete subgroup $S(1080)$. Using a modified action that allows classical simulations down to $a \approx 0.08$ fm, the low-lying glueball spectrum is computed with percent-level precision at multiple lattice spacings and shown to extrapolate to the continuum limit $SU(3)$ results. This suggests that this digitization scheme is sufficient for precision quantum simulations of QCD.

Introduction — Numerous observables remain firmly beyond the reach of numerical nonperturbative field theory [1–3] due to the sign problem. Sign problems arise when the imaginary time (euclidean) action of the system is complex or when a real time representation is required. Finite density problems (like the calculation of the equation of state of dense QCD matter or the Hubbard model away from half-filling) are famous examples of the first case; thermalization is an example of the second.

Due to the importance of these problems much effort has been spent on solving or bypassing the sign problem. Quantum computers are a promising avenue leading to a solution to these problems. The time development of the quantum system can be directly mapped into the time evolution of the quantum computer obviating the need for imaginary time calculations. The subtle interference patterns appearing on real time evolution are mimicked by the same pattern inside the quantum computer.

Besides the obvious technological difficulty of building quantum computers, conceptual questions must be answered before quantum field theory can be simulated. First, the state of the system needs to be mapped into a finite – and likely small – quantum register. Then the initial state needs to be prepared, the hamiltonian evolution coded in terms of elementary gates and, finally, observables must be measured. This paper focuses on the first step, the encoding of the states in the quantum register. The difficulty arises mainly in bosonic theories. Indeed, purely fermionic theories have an infinite dimensional Hilbert space but the usual discretization of space into a finite lattice suffices to reduce the dimensionality to a finite number mappable into a quantum register. However, the Hilbert space of a bosonic fields defined in a single lattice point is already infinite dimensional. Thus, further discretization of *field space* is required to map bosons into a digital quantum register. A wide array of solutions

exist [4–14]. Different digitizations break different symmetries of the model [5, 7, 15]. With these reductions, the universality class of the lattice model may differ from the original theory [16–23] making the continuum space limit problematic. Recently, studies quantified the truncation errors for quantum simulations of lattice theories from a computational complexity perspective [12, 24–26].

Here, we will investigate the discrete subgroup approximation [27–30] using classical lattice simulations. While performed in imaginary time, this nonperturbative study of truncation errors is known to be related to those in real time [31–33], thus providing us access to much larger systems than with current quantum devices. Discrete subgroups were studied in the early days of lattice field theory when memory limitations restricted the feasible lattice volumes due to the cost of storing $SU(3)$ elements.

Replacing a continuous symmetry with a discrete (and smaller) may easily destroy the proper (spacetime) continuum limit. In asymptotically free theories like QCD, the continuum limit is obtained as the inverse coupling β diverges while the lattice spacing a goes to zero. However, for a smaller than a certain threshold a_f the discrete theory differs drastically from the one with a continuous group (although there are counterexamples [34]). In the language of euclidean path integrals, the field configurations are “frozen” on the configurations with the minimal action, with the other configurations, due to the gap in action, being exponentially suppressed. This freezing is not necessarily fatal provided we reach the scaling regime: realistic lattice calculations are performed on classical computers with a finite a and extrapolated to $a \rightarrow 0$. In these calculations, a should be smaller than typical hadronic scales with modern values of $\mathcal{O}(0.1$ fm).

Subgroups of $U(1)$ [35–37] and $SU(N)$ [38–45] gauge fields – including with fermions [46, 47] – were tested with differing degrees of success. In particular, all five crystal-like subgroups of $SU(3)$ freeze before the scaling regime with the Wilson action [28, 40, 42]. Subsequent work increased the phase transition by including the mid-points between elements of $S(1080)$ [43]. However, this procedure breaks gauge symmetry. An alternative proposal studied for $U(1)$ chooses an optimized subset of

* aalexan@gwu.edu

† bedaque@umd.edu

‡ rbrett@gwu.edu

§ hlamm@fnal.gov

group elements [48, 49].

Introducing new terms to the discrete action can decrease a_f . The new action has formally the same continuum limit, but it is different at finite lattice spacing. The net effect is that the gap δS between the lowest action configurations is lowered and the freezing a_f is reduced. Classical Monte Carlo calculations were performed in [28], finding that $a \approx 0.08$ fm is possible with the addition of a single term to the action. We must check empirically that this action generates the same physics as $SU(3)$ by reproducing continuum IR observables. The previous work [28] demonstrated that the deconfining temperature of pure-gluon $SU(3)$ was reproduced in the continuum from $S(1080)$ to sub-percent accuracy. In order to argue for the usefulness of this approach to quantum simulations we need verify that the $S(1080)$ is capable of reproducing the hadronic spectrum. Here, we show that percent-level accuracy can be achieved for the low-lying glueball states, the massive excitations of pure-gluon $SU(3)$.

Theory — In this work, we use the action proposed in [28]:

$$S[U] = - \sum_p \left(\frac{\beta_0}{3} \text{Re Tr}(U_p) + \beta_1 \text{Re Tr}(U_p^2) \right), \quad (1)$$

where U_p is a plaquette and β_i are coupling constants. Modified actions like Eq. (1) were observed for $U_p \in SU(3)$ to have milder lattice spacing errors [50–54] with the same continuum limit as the Wilson action ($S_W = -\frac{\beta_W}{3} \sum_p \text{Re Tr} U_p$).

The inability of the discrete field fluctuations to be made arbitrarily small lead to a phase boundary $\{\beta_i\}$ beyond which $S(1080)$ gauge links become frozen to $\mathbb{1}$ while the $SU(3)$ gauge links remain dynamical. In this phase, no clear connection between $S(1080)$ and $SU(3)$ exists. That is what limits the lattice spacing to $a > a_f$. By setting $\beta_1 < 0$ the gap between the values of the frozen and dynamical discrete links is reduced and thus a_f decreased.

In [28] the trajectory $\beta_1 = -0.1267\beta_0 + 0.253$ was found to allow for lattice spacing down to $a \gtrsim 0.08$ fm when computing the Wilson flow parameter t_0 [55]. This trajectory was chosen to avoid the freezing transition in a small 2^4 lattice. This value of $a \gtrsim 0.08$ fm is clearly in the scaling regime where the correlation lengths are much smaller than a and lattice artifacts are small.

Methodology — To extract glueball masses we need to measure two-point functions of operators with the appropriate quantum numbers. Gluon correlators are noisy and the extraction of gluon masses hinge on a good choice of interpolating fields and a variational calculation employing a large set of operators. Fortunately, a sophisticated technique has been developed that we can use for glueball spectroscopy [56–61]. While the traditional approach for $SU(3)$ glueball spectroscopy involves anisotropic lattices [58], we used isotropic lattices, to

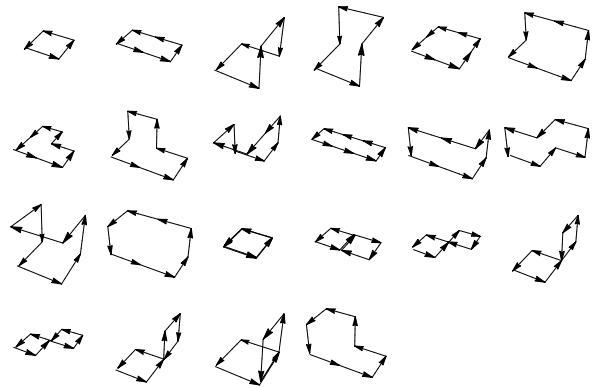


FIG. 1. Seed loops for the operator constructions, using 4, 6, and 8 links.

avoid the complication of tuning the anisotropy. These operators need to be gauge invariant and are constructed from traces of *loops*, sets of links that track paths that return to the starting point. The basic seed paths we used for this study are one 4-link long, three 6-link long, and 18 8-links long (Fig. 1). Generically an n -link loop operator is given by

$$[x; \mu_1, \dots, \mu_n] \equiv \text{Tr} \prod_{i=1}^n U_{\mu_i} \left(x + \sum_{j<i} \mu_j \right). \quad (2)$$

Above, x is the starting point for the loop and μ_i are *spatial* displacements for the loop. Since this is a loop, the displacements satisfy $\sum_k \mu_k = 0$. The *links* $U_\mu(x)$ represent a Wilson line connecting x and $x + \mu$. As the lattice spacing is reduced the loops are enlarged by *blocking*, that is, repeating the steps in the loop, so that the size of the loops in physical units stays constant. For example $[\mu_1, \mu_2, \dots, \mu_n]$ can be replaced with $[\mu_1, \mu_1, \mu_2, \mu_2, \dots, \mu_n, \mu_n]$.

We will consider only zero-momentum operators resulting from summing (2) over x . These operators have symmetries that we use to make their calculation more efficient: they are invariant under circular permutations of the steps, and the opposite orientation loop is related to the original one via a complex-conjugation.

The loop operators must be projected onto the appropriate irreducible representations (*irreps*) of the finite-volume symmetry group O_h (we consider only cubic boxes), a subgroup of the infinite-volume symmetry group, $O(3)$. These projectors are given by:

$$P_{\lambda\lambda'}^\Gamma \ell \equiv \frac{d_\Gamma}{|G|} \sum_{g \in G} [D_{\lambda\lambda'}^\Gamma(g)]^* R(g) \ell, \quad (3)$$

where $\ell = [\mu_1, \dots, \mu_n]$ and $R\ell = [R\mu_1, \dots, R\mu_n]$ is the loop transformed by R . Above, d_Γ is the dimension of the irrep Γ , $|G|$ is the number of elements in the group, $D^\Gamma(g)$ is the matrix associated with element g in irrep Γ

and $R(g)$ is the three-dimensional representation of O_h (these are the same matrices as $D^{T_1^-}(g)$.) The group O_h has 24 proper rotations, and 24 rotations combined with an inversion. There are 10 irreps: A_1^\pm , A_2^\pm , E^\pm , T_1^\pm , and T_2^\pm with dimensions 1, 1, 2, 3, and 3. The multiplets of $O(3)$ can be decomposed into smaller invariant multiplets of O_h . For instance, the scalar ($J = 0$) irrep corresponds to the A_1 irrep of O_h while the $J = 2$ breaks down into $E \oplus T_2$. The parity are the same for both infinite volume and finite volume irreps.

The other quantum number relevant for operator construction is the charge parity. Charge conjugation for the glue fields is given by $U_\mu(x) \rightarrow U_\mu(x)^*$, so the loop operators transform similarly $\ell \rightarrow \ell^*$. The even-charge operators, which we consider here, correspond to the real part of ℓ and the odd ones to the imaginary parts. Finally, in order to increase the overlap of the loop-operators with the glueball states we *stout smear* the links [62].

In our calculation, we used the following operator basis. All loops were computed using smeared operator on blocked links. We used 16 different combinations. For each gauge-configuration we repeatedly smeared the links generating four different smearing levels with $n_{\text{smear}} = 2, 4, 6, 8$. For each smearing set of links we evaluated the loops using blocked links with $n_{\text{block}} = 2, 4, 6, 8$.

Since the gluon correlators becomes noisy at fairly small time separations, a delicate fitting procedure is required to extract the glueball masses. Finite-volume glueball energies are best extracted by computing matrices of temporal correlators,

$$C_{ij}(\tau) = \sum_{\tau_0} \langle 0 | \mathcal{O}_i(\tau + \tau_0) \mathcal{O}_j(\tau_0)^\dagger | 0 \rangle, \quad (4)$$

for large sets of glueball operators $\mathcal{O}(\tau) = O(\tau) - \langle 0 | O(\tau) | 0 \rangle$. In practice, the vacuum subtraction only needs to be performed for operators with vacuum quantum numbers, i.e. the A_1^{++} sector. We construct the matrix

$$\tilde{C}(\tau) = U^\dagger C(\tau_0)^{-1/2} C(\tau) C(\tau_0)^{-1/2} U, \quad (5)$$

where the columns of U are the eigenvectors of $G(\tau_d) = C(\tau_0)^{-1/2} C(\tau_d) C(\tau_0)^{-1/2}$. The parameters τ_0 and τ_d , named the pivot and diagonalization times, are chosen such that $\tilde{C}(\tau)$ remains (approximately) diagonal for $\tau > \tau_d$, and the extracted energies are insensitive to parameter variations. The spectrum is then extracted by fitting the diagonal elements $\tilde{C}_{kk}(\tau)$ to the ansatz $A_k [e^{-E_k \tau} + e^{-E_k(T-\tau)}]$, with T the extent of the Euclidean lattice time. The ground state is associated with the largest eigenvalue of $G(\tau_d)$, the first excited state with the second largest eigenvalue, and so on.

From the 22 seed loops in Fig. 1, 626 linearly independent operators are produced across the $20 \Gamma^C$ symmetry sectors. Performing the smearing and blocking process leads to 10,016 independent operators for the 16 sets of

links. While the full set of operators for a given irrep can be used, in practice it is often necessary to carefully prune the operator basis. This is done by removing operators with poor overlap onto the states of interest, and those whose correlators have a low signal-to-noise ratio. Unlike modern QCD calculations [63, 64] here we are only interested in the ground state in a given irrep. Therefore, while pruning is helpful in simplifying the analysis to smaller matrices, we find our results insensitive to it.

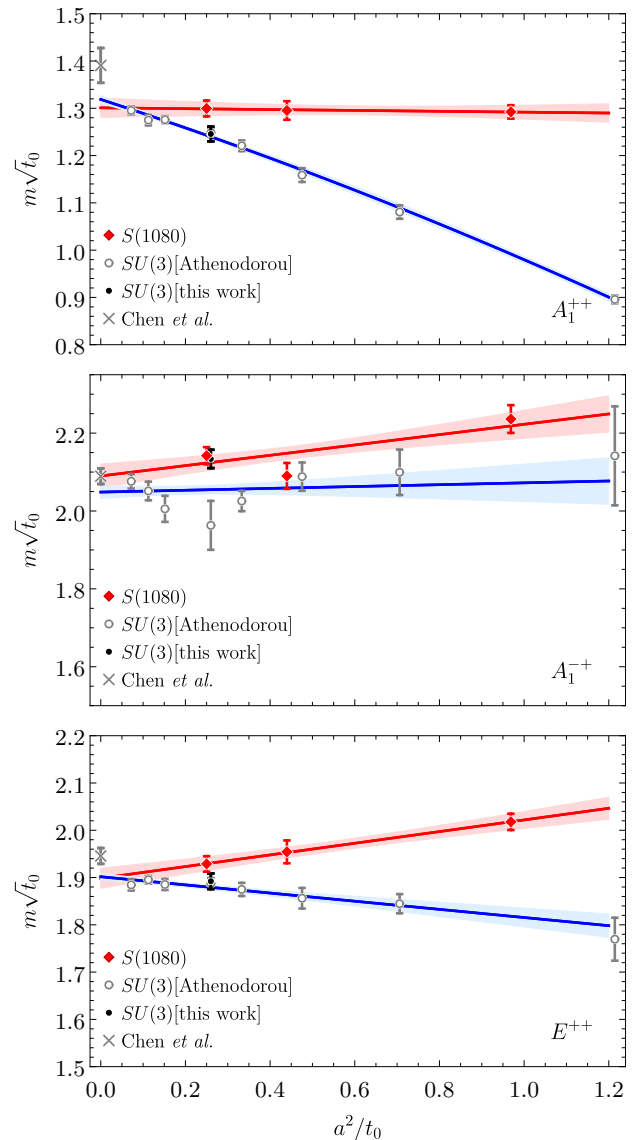


FIG. 2. Masses for A_1^{++} ($J^{PC} = 0^{++}$), A_1^{-+} ($J^{PC} = 0^{-+}$), and E^{++} ($J^{PC} = 2^{++}$) glueballs vs a^2/t_0 . Our $S(1080)$ (\blacklozenge) and $SU(3)$ (\bullet) results compared to $SU(3)$ results from [61] (\circ). Another continuum $SU(3)$ result [60] (\times) is presented to estimate systematic errors.

Results — Our results are obtained from three $S(1080)$ ensembles using the same couplings as [28]. The parameters were chosen to scan a set $a \in [0.08, 0.16]$ fm. The

lattice spacing was determined from t_0 , the Wilson flow time [55]. A detailed list of parameters is in Table I. These ensembles were generated using a multi-hit Metropolis update algorithm, which we found to be as efficient as a heat-bath in terms of autocorrelation length but significantly cheaper to implement. For each ensemble we generated around 650,000 independent configurations with sufficient decorrelation steps. Computing time was dominated by measuring the loop-operators, so we used a conservative number of update steps between measurements.

To verify that our operator basis overlaps well with the glueballs and that our fitting method is sound, we carried out a calibration run using an $SU(3)$ ensemble. We generated a set of $SU(3)$ Wilson-gauge configurations for $\beta = 6.0625$ and compare our results with the state-of-the-art calculations of [61] for one value of β that is near the lattice spacing on one of our $S(1080)$ ensembles. We generated similar statistics to the $S(1080)$ ensembles and used the same set of operators. The full set of parameters for this run is included in the last row of Table I.

For analysis we binned the measurements in groups of 500, both to remove the possible autocorrelation effects and to make the data analysis more manageable. We fit a single exponential function, $A[e^{-m\tau} + e^{-m(T-\tau)}]$, to the ground state correlator in the time range $\tau \in [\tau_i, \tau_f]$. The relevant parameters for these calculations are in Table II. The masses and their errors were extracted using a correlated fit to take into account the covariance of the correlator at different times. The covariance matrix for the correlator was estimated using the jackknife method. The results are plotted in Fig. 2 and included in Table I.

We extracted the glueball masses corresponding to the ground states in the A_1^{++} , E^{++} , and A_1^{-+} irreps, corresponding to the lowest lying glueballs. The $SU(3)$ calibration run results are included in Fig. 2 and are consistent with those from Ref. [61]. The A_1^{-+} point differs from the corresponding mass from Ref. [61], yet we note that at this point the results from Ref. [61] have large error-bars and are at tension with their own continuum extrapolation. Our $S(1080)$ results are extrapolated to $a = 0$ assuming the expected quadratic form $m(a)\sqrt{t_0} = m(0)\sqrt{t_0} + ca^2/t_0$. These extrapolations are indicated in Fig. 2 with a red line and compared with the $SU(3)$ extrapolations from Refs. [60, 61]. For our calculations we use $\sqrt{t_0}/a$ values measured directly on these ensembles [28] (see Table I). For the $SU(3)$ results we used the parameterization of $\sqrt{t_0}/a$ as a function of β for the pure glue Wilson action included in a recent study [65] and we perform the same continuum extrapolation as in Ref. [61]. To gauge the systematics of the $SU(3)$ calculation, we included the results from an independent calculation [60]. The extrapolation results are included in Table III. As we can see, the results agree within their statistical errors at the percent level. Compared to previous results for the deconfining temperature $T_0\sqrt{t_0} = 0.2489(11)$, our results probe nearly an order of magnitude higher in energy $m\sqrt{t_0} \sim 2$

finding agreement with $SU(3)$ in the continuum. This supports the claim that this modified action reproduces $SU(3)$ physics below 2.5 GeV^{-1} .

Conclusions — These results provides strong evidence that $S(1080)$ can replace $SU(3)$ in quantum simulations of observables which cannot be computed using classical lattice techniques in imaginary time e.g. [66]. This includes some key QCD phenomena that have remained mysterious up to now like the mechanism of thermalization in heavy ion collisions that is believed to be driven mostly by gluons. The $\mathcal{O}(10^2)$ qubit savings from using an 11-qubit $S(1080)$ register instead of $SU(3)$ compare favorably to other digitizations [14, 67–70]. Even with the small lattice sizes dominating the error due to the limited number of qubits, the model studied here represents a sufficient approximation of $SU(3)$ for $a \gtrsim 0.08$ fm. As quantum computers get larger, smaller lattice errors may become desirable. In such case, systematic improvements are possible. Including additional terms in the action proportional to other characters [29, 44, 45] can allow for smaller a , while improved actions, in the spirit of the Symanzik program, can reduce the systemic error for fixed a [71–73]. The relative cost of these two improvements are left for future work. Finally, including dynamical fermions into discrete subgroups simulations should be performed to understand how this full theory compared to QCD. While there is no conceptual issue in including fermions, the numerical value of the minimum lattice size achievable will depend on the number of dynamical quarks.

A.A. and R.B. are grateful to Andreas Athenodorou for his guidance on constructing a good operator basis for the variational analysis. P.B was supported in part by the US DoE under contract No. DE-FG02-93ER-40762 and by U.S. DOE Grant No. DE-SC0021143. A.A. is supported in part by the U.S. Department of Energy grant DE-FG02-95ER40907. H.L is supported by the Department of Energy through the Fermilab QuantiSED program in the area of “Intersections of QIS and Theoretical Particle Physics”. Fermilab is operated by Fermi Research Alliance, LLC under contract number DE-AC02-07CH11359 with the United States Department of Energy.

-
- [1] R. P. Feynman, Simulating physics with computers, *Int. J. Theor. Phys.* **21**, 467 (1982).
 - [2] S. P. Jordan, H. Krovi, K. S. Lee, and J. Preskill, BQP-completeness of Scattering in Scalar Quantum Field Theory, *Quantum* **2**, 44 (2018), arXiv:1703.00454 [quant-ph].
 - [3] M. Carena, H. Lamm, Y.-Y. Li, J. D. Lykken, L.-T. Wang, and Y. Yamauchi, Practical Quantum Advantages in High Energy Physics, *Snowmass 2021 LOI TF10-077* (2020).
 - [4] E. Zohar, J. I. Cirac, and B. Reznik, Cold-Atom Quantum Simulator for $SU(2)$ Yang-Mills Lattice Gauge Theory, *Phys. Rev. Lett.* **110**, 125304 (2013), arXiv:1211.2241

TABLE I. Input parameters. The top three lines are for $S(1080)$ and the forth is the $SU(3)$ calibration run. The parameters are: ρ the stout smearing parameter, n_{decorr} the number of updates between measurements, n_ρ and n_b the number of smearing and blocking levels respectively. For $S(1080)$, the couplings β_0 and β_1 are normalized as in Eq. (1), and follow the trajectory in the text, whereas for $SU(3)$ simulations β_0 is the Wilson coupling. Observables are quoted in lattice units, with statistical errors only. For $SU(3)$ the value of $\sqrt{t_0}/a$ is from [65].

β_0	β_1	$n_x^3 \times n_t$	n_{therm}	n_{decorr}	ρ	n_{meas}	n_{bins}	$\sqrt{t_0}/a$	$am_{A_1^{++}}$	$am_{A_1^{-+}}$	$am_{E^{++}}$
9.154	-0.9065	$16^3 \times 16$	200	40	0.2	652500	1305	1.016(3)	1.272(14)	2.201(35)	1.986(17)
12.795	-1.3677	$16^3 \times 16$	200	40	0.2	650000	1300	1.508(3)	0.859(13)	1.386(22)	1.296(16)
19.61	-2.2309	$16^3 \times 16$	200	40	0.2	647500	1295	2.000(4)	0.6498(84)	1.071(11)	0.9644(82)
6.0625	—	$16^3 \times 16$	200	5	0.2	567500	1135	1.962(1)	0.6352(79)	1.088(12)	0.9649(84)

TABLE II. Analysis parameters for the $S(1080)$ calculation (top rows) and the $SU(3)$ calibration run (bottom). Included are the pivot time τ_0 , the diagonalization time τ_d , the fit range $[\tau_i, \tau_f]$, and the χ^2 per degree of freedom.

β_0	irrep	τ_0	τ_d	τ_i	τ_f	χ^2/dof
9.154	A_1^{++}	0	1	2	7	0.94
	A_1^{-+}	1	2	1	15	0.82
	E^{++}	0	1	1	15	1.37
12.795	A_1^{++}	0	1	3	8	1.24
	A_1^{-+}	0	1	2	7	0.96
	E^{++}	0	1	2	8	1.91
19.61	A_1^{++}	0	1	3	8	1.47
	A_1^{-+}	0	1	2	5	1.11
	E^{++}	0	1	2	8	0.83
6.0625	A_1^{++}	2	3	3	10	1.01
	A_1^{-+}	0	1	2	7	0.90
	E^{++}	1	2	2	8	1.07

TABLE III. $a \rightarrow 0$ extrapolations of $m\sqrt{t_0}$, for $S(1080)$ and $SU(3)$ simulations. The results of [61] uses an isotropic lattice whereas [60] use an anisotropic lattice.

irrep	$S(1080)$	$SU(3)$ [61]	$SU(3)$ [60]
A_1^{++}	1.301(20)	1.319(8)	1.391(37)
A_1^{-+}	2.090(31)	2.049(17)	2.089(20)
E^{++}	1.899(21)	1.902(7)	1.946(17)

[quant-ph].

- [5] E. Zohar, J. I. Cirac, and B. Reznik, Quantum simulations of gauge theories with ultracold atoms: local gauge invariance from angular momentum conservation, *Phys. Rev. A* **88**, 023617 (2013), arXiv:1303.5040 [quant-ph].
- [6] E. Zohar and M. Burrello, Formulation of lattice gauge theories for quantum simulations, *Phys. Rev. D* **91**, 054506 (2015), arXiv:1409.3085 [quant-ph].
- [7] U.-J. Wiese, Towards Quantum Simulating QCD, *Proceedings, 24th International Conference on Ultra-Relativistic Nucleus-Nucleus Collisions (Quark Matter 2014): Darmstadt, Germany, May 19-24, 2014*, *Nucl. Phys. A* **931**, 246 (2014), arXiv:1409.7414 [hep-th].
- [8] E. Zohar, A. Farace, B. Reznik, and J. I. Cirac, Digital lattice gauge theories, *Phys. Rev. A* **95**, 023604 (2017), arXiv:1607.08121 [quant-ph].
- [9] J. Bender, E. Zohar, A. Farace, and J. I. Cirac, Digital quantum simulation of lattice gauge theories in three spatial dimensions, *New J. Phys.* **20**, 093001 (2018), arXiv:1804.02082 [quant-ph].
- [10] N. Klco, J. R. Stryker, and M. J. Savage, $SU(2)$ non-Abelian gauge field theory in one dimension on digital quantum computers, *Phys. Rev. D* **101**, 074512 (2020), arXiv:1908.06935 [quant-ph].
- [11] I. Raychowdhury and J. R. Stryker, Loop, String, and Hadron Dynamics in $SU(2)$ Hamiltonian Lattice Gauge Theories, *Phys. Rev. D* **101**, 114502 (2020), arXiv:1912.06133 [hep-lat].
- [12] Z. Davoudi, I. Raychowdhury, and A. Shaw, Search for Efficient Formulations for Hamiltonian Simulation of non-Abelian Lattice Gauge Theories (2020), arXiv:2009.11802 [hep-lat].
- [13] M. Kreshchuk, W. M. Kirby, G. Goldstein, H. Beauchemin, and P. J. Love, Quantum Simulation of Quantum Field Theory in the Light-Front Formulation (2020), arXiv:2002.04016 [quant-ph].
- [14] A. Ciavarella, N. Klco, and M. J. Savage, A Trailhead for Quantum Simulation of $SU(3)$ Yang-Mills Lattice Gauge Theory in the Local Multiplet Basis (2021), arXiv:2101.10227 [quant-ph].
- [15] I. Raychowdhury and J. R. Stryker, Solving Gauss's Law on Digital Quantum Computers with Loop-String-Hadron Digitization, *Phys. Rev. Res.* **2**, 033039 (2020), arXiv:1812.07554 [hep-lat].
- [16] P. Hasenfratz and F. Niedermayer, Asymptotic freedom with discrete spin variables?, *Proceedings, 2001 Europhysics Conference on High Energy Physics (EPS-HEP 2001): Budapest, Hungary, July 12-18, 2001*, *PoS HEP2001*, 229 (2001), arXiv:hep-lat/0112003 [hep-lat].
- [17] S. Caracciolo, A. Montanari, and A. Pelissetto, Asymptotically free models and discrete nonAbelian groups, *Phys. Lett. B* **513**, 223 (2001), arXiv:hep-lat/0103017 [hep-lat].
- [18] P. Hasenfratz and F. Niedermayer, Asymptotically free theories based on discrete subgroups, *Lattice field theory. Proceedings, 18th International Symposium, Lattice 2000, Bangalore, India, August 17-22, 2000*, *Nucl. Phys. Proc. Suppl.* **94**, 575 (2001), arXiv:hep-lat/0011056 [hep-lat].
- [19] A. Patrascioiu and E. Seiler, Continuum limit of two-dimensional spin models with continuous symmetry and conformal quantum field theory, *Phys. Rev. E* **57**, 111 (1998).
- [20] R. Krccmar, A. Gendiar, and T. Nishino, Phase diagram of a truncated tetrahedral model, *Phys. Rev. E* **94**, 022134 (2016).
- [21] A. Alexandru, P. F. Bedaque, H. Lamm, and S. Lawrence

- (NuQS), σ Models on Quantum Computers, *Phys. Rev. Lett.* **123**, 090501 (2019), [arXiv:1903.06577 \[hep-lat\]](#).
- [22] S. Caracciolo, A. Montanari, and A. Pelissetto, Asymptotically free models and discrete non-abelian groups, *Physics Letters B* **513**, 223 (2001).
- [23] A. Alexandru, P. F. Bedaque, A. Carosso, and A. Sheng, Universality of a truncated sigma-model (2021), [arXiv:2109.07500 \[hep-lat\]](#).
- [24] A. F. Shaw, P. Lougovski, J. R. Stryker, and N. Wiebe, Quantum Algorithms for Simulating the Lattice Schwinger Model, *Quantum* **4**, 306 (2020), [arXiv:2002.11146 \[quant-ph\]](#).
- [25] A. Kan and Y. Nam, Lattice Quantum Chromodynamics and Electrodynamics on a Universal Quantum Computer (2021), [arXiv:2107.12769 \[quant-ph\]](#).
- [26] Y. Tong, V. V. Albert, J. R. McClean, J. Preskill, and Y. Su, Provably accurate simulation of gauge theories and bosonic systems (2021), [arXiv:2110.06942 \[quant-ph\]](#).
- [27] D. C. Hackett, K. Howe, C. Hughes, W. Jay, E. T. Neil, and J. N. Simone, Digitizing Gauge Fields: Lattice Monte Carlo Results for Future Quantum Computers, *Phys. Rev. A* **99**, 062341 (2019), [arXiv:1811.03629 \[quant-ph\]](#).
- [28] A. Alexandru, P. F. Bedaque, S. Harmalkar, H. Lamm, S. Lawrence, and N. C. Warrington (NuQS), Gluon field digitization for quantum computers, *Phys.Rev.D* **100**, 114501 (2019), [arXiv:1906.11213 \[hep-lat\]](#).
- [29] Y. Ji, H. Lamm, and S. Zhu (NuQS), Gluon Field Digitization via Group Space Decimation for Quantum Computers, *Phys. Rev. D* **102**, 114513 (2020), [arXiv:2005.14221 \[hep-lat\]](#).
- [30] M. S. Alam, S. Hadfield, H. Lamm, and A. C. Y. Li, Quantum Simulation of Dihedral Gauge Theories (2021), [arXiv:2108.13305 \[quant-ph\]](#).
- [31] K. Osterwalder and R. Schrader, Axioms for Euclidean Green's Functions, *Commun. Math. Phys.* **31**, 83 (1973).
- [32] K. Osterwalder and R. Schrader, Axioms for Euclidean Green's Functions. 2., *Commun. Math. Phys.* **42**, 281 (1975).
- [33] M. Carena, H. Lamm, Y.-Y. Li, and W. Liu, Lattice Renormalization of Quantum Simulations (2021), [arXiv:2107.01166 \[hep-lat\]](#).
- [34] B. B. Beard, M. Pepe, S. Riederer, and U. J. Wiese, Study of CP(N-1) theta-vacua by cluster-simulation of SU(N) quantum spin ladders, *Phys. Rev. Lett.* **94**, 010603 (2005), [arXiv:hep-lat/0406040 \[hep-lat\]](#).
- [35] M. Creutz, L. Jacobs, and C. Rebbi, Monte Carlo Study of Abelian Lattice Gauge Theories, *Phys. Rev.* **D20**, 1915 (1979).
- [36] M. Creutz and M. Okawa, Generalized Actions in $Z(p)$ Lattice Gauge Theory, *Nucl. Phys.* **B220**, 149 (1983).
- [37] M. Fukugita, T. Kaneko, and M. Kobayashi, Phase Structure and Duality of $Z(N)$ Lattice Gauge Theory With Generalized Actions in Four Space-time Dimensions, *Nucl. Phys. B* **215**, 289 (1983).
- [38] D. Petcher and D. H. Weingarten, Monte Carlo Calculations and a Model of the Phase Structure for Gauge Theories on Discrete Subgroups of SU(2), *Phys. Rev.* **D22**, 2465 (1980).
- [39] L. Jacobs and C. Rebbi, Multispin Coding: A Very Efficient Technique for Monte Carlo Simulations of Spin Systems, *J. Comput. Phys.* **41**, 203 (1981).
- [40] G. Bhanot and C. Rebbi, Monte Carlo Simulations of Lattice Models With Finite Subgroups of SU(3) as Gauge Groups, *Phys. Rev.* **D24**, 3319 (1981).
- [41] H. Grosse and H. Kuhnelt, Phase Structure of Lattice Gauge Theories for Nonabelian Subgroups of SU(3), *Phys. Lett.* **101B**, 77 (1981).
- [42] G. Bhanot, SU(3) Lattice Gauge Theory in Four-dimensions With a Modified Wilson Action, *Phys. Lett.* **108B**, 337 (1982).
- [43] P. Lisboa and C. Michael, Discrete Subsets of SU(3) for Lattice Gauge Theory, *Phys. Lett.* **113B**, 303 (1982).
- [44] H. Flyvbjerg, Group Space Decimation: A Way to Simulate the 1080 Element Subgroup of SU(3)?, *Nucl. Phys.* **B243**, 350 (1984).
- [45] H. Flyvbjerg, Internal Space Decimation for Lattice Gauge Theories, *Nucl. Phys.* **B240**, 481 (1984).
- [46] D. H. Weingarten and D. N. Petcher, Monte Carlo Integration for Lattice Gauge Theories with Fermions, *Phys. Lett.* **99B**, 333 (1981).
- [47] D. Weingarten, Monte Carlo Evaluation of Hadron Masses in Lattice Gauge Theories with Fermions, *Phys. Lett.* **109B**, 57 (1982), [631(1981)].
- [48] J. F. Haase, L. Dellantonio, A. Celi, D. Paulson, A. Kan, K. Jansen, and C. A. Muschik, A resource efficient approach for quantum and classical simulations of gauge theories in particle physics (2020), [arXiv:2006.14160 \[quant-ph\]](#).
- [49] C. W. Bauer and D. M. Grabowska, Efficient Representation for Simulating U(1) Gauge Theories on Digital Quantum Computers at All Values of the Coupling (2021), [arXiv:2111.08015 \[hep-ph\]](#).
- [50] T. Blum, C. E. DeTar, U. M. Heller, L. Karkkainen, K. Rummukainen, and D. Toussaint, Thermal phase transition in mixed action SU(3) lattice gauge theory and Wilson fermion thermodynamics, *Nucl. Phys.* **B442**, 301 (1995), [arXiv:hep-lat/9412038 \[hep-lat\]](#).
- [51] U. M. Heller, SU(3) lattice gauge theory in the fundamental adjoint plane and scaling along the Wilson axis, *Phys. Lett.* **B362**, 123 (1995), [arXiv:hep-lat/9508009 \[hep-lat\]](#).
- [52] U. M. Heller, More on SU(3) lattice gauge theory in the fundamental adjoint plane, *Lattice '95. Proceedings, International Symposium on Lattice Field Theory, Melbourne, Australia, July 11-15, 1995*, *Nucl. Phys. Proc. Suppl.* **47**, 262 (1996), [arXiv:hep-lat/9509010 \[hep-lat\]](#).
- [53] M. Hasenbusch and S. Necco, Lattice artefacts in SU(3) lattice gauge theory with a mixed fundamental and adjoint plaquette action, *Lattice field theory. Proceedings, 22nd International Symposium, Lattice 2004, Batavia, USA, June 21-26, 2004*, *Nucl. Phys. Proc. Suppl.* **140**, 743 (2005), [arXiv:hep-lat/0409067 \[hep-lat\]](#).
- [54] M. Hasenbusch and S. Necco, SU(3) lattice gauge theory with a mixed fundamental and adjoint plaquette action: Lattice artifacts, *JHEP* **08**, 005, [arXiv:hep-lat/0405012 \[hep-lat\]](#).
- [55] Lüscher, Martin, Properties and uses of the Wilson flow in lattice QCD, *JHEP* **08**, 071, [Erratum: *JHEP*03,092(2014)], [arXiv:1006.4518 \[hep-lat\]](#).
- [56] B. Berg and A. Billoire, Glueball Spectroscopy in Four-dimensional SU(3) Lattice Gauge Theory. 1., *Nucl. Phys. B* **221**, 109 (1983).
- [57] B. Berg and A. Billoire, Glueball Spectroscopy in Four-dimensional SU(3) Lattice Gauge Theory. 2., *Nucl. Phys. B* **226**, 405 (1983).
- [58] C. J. Morningstar and M. J. Peardon, The Glueball spectrum from an anisotropic lattice study, *Phys. Rev.* **D60**, 034509 (1999), [arXiv:hep-lat/9901004 \[hep-lat\]](#).
- [59] U. Wenger, *Lattice Gauge Theory with Fixed Point Ac-*

- tions, Ph.D. thesis, Universität Bern (2000).
- [60] Y. Chen *et al.*, Glueball spectrum and matrix elements on anisotropic lattices, *Phys. Rev.* **D73**, 014516 (2006), [arXiv:hep-lat/0510074 \[hep-lat\]](#).
- [61] A. Athenodorou and M. Teper, The glueball spectrum of SU(3) gauge theory in 3 + 1 dimensions, *JHEP* **11**, 172, [arXiv:2007.06422 \[hep-lat\]](#).
- [62] C. Morningstar and M. J. Peardon, Analytic smearing of SU(3) link variables in lattice QCD, *Phys. Rev.* **D69**, 054501 (2004), [arXiv:hep-lat/0311018 \[hep-lat\]](#).
- [63] R. Brett, J. Bulava, D. Darvish, J. Fallica, A. Hanlon, B. Hörz, and C. Morningstar, Spectroscopy From The Lattice: The Scalar Glueball, *AIP Conf. Proc.* **2249**, 030032 (2020), [arXiv:1909.07306 \[hep-lat\]](#).
- [64] C. Culver, M. Mai, R. Brett, A. Alexandru, and M. Döring, Three pion spectrum in the $I = 3$ channel from lattice QCD, *Phys. Rev. D* **101**, 114507 (2020), [arXiv:1911.09047 \[hep-lat\]](#).
- [65] A. Francis, O. Kaczmarek, M. Laine, T. Neuhaus, and H. Ohno, Critical point and scale setting in SU(3) plasma: An update, *Phys. Rev.* **D91**, 096002 (2015), [arXiv:1503.05652 \[hep-lat\]](#).
- [66] T. D. Cohen, H. Lamm, S. Lawrence, and Y. Yamauchi, Quantum algorithms for transport coefficients in gauge theories (2021), [arXiv:2104.02024 \[hep-lat\]](#).
- [67] D. Banerjee, M. Dalmonte, M. Muller, E. Rico, P. Stebler, U. J. Wiese, and P. Zoller, Atomic Quantum Simulation of Dynamical Gauge Fields coupled to Fermionic Matter: From String Breaking to Evolution after a Quench, *Phys. Rev. Lett.* **109**, 175302 (2012), [arXiv:1205.6366 \[cond-mat.quant-gas\]](#).
- [68] D. Banerjee, M. Bögli, M. Dalmonte, E. Rico, P. Stebler, U. J. Wiese, and P. Zoller, Atomic Quantum Simulation of U(N) and SU(N) Non-Abelian Lattice Gauge Theories, *Phys. Rev. Lett.* **110**, 125303 (2013), [arXiv:1211.2242 \[cond-mat.quant-gas\]](#).
- [69] D. Marcos, P. Widmer, E. Rico, M. Hafezi, P. Rabl, U. J. Wiese, and P. Zoller, Two-dimensional Lattice Gauge Theories with Superconducting Quantum Circuits, *Annals Phys.* **351**, 634 (2014), [arXiv:1407.6066 \[quant-ph\]](#).
- [70] E. Rico, M. Dalmonte, P. Zoller, D. Banerjee, M. Bögli, P. Stebler, and U. J. Wiese, SO(3) "Nuclear Physics" with ultracold Gases, *Annals Phys.* **393**, 466 (2018), [arXiv:1802.00022 \[cond-mat.quant-gas\]](#).
- [71] K. Symanzik, Continuum Limit and Improved Action in Lattice Theories. 1. Principles and ϕ^4 Theory, *Nucl. Phys. B* **226**, 187 (1983).
- [72] M. Luscher and P. Weisz, On-Shell Improved Lattice Gauge Theories, *Commun. Math. Phys.* **97**, 59 (1985), [Erratum: *Commun. Math. Phys.* 98,433(1985)].
- [73] M. Luscher and P. Weisz, Computation of the Action for On-Shell Improved Lattice Gauge Theories at Weak Coupling, *Phys. Lett. B* **158**, 250 (1985).